LA-UR- 96- 1206

CONF-960412--3

Title: Prototype Explosives Detection System Based on Nuclear Resonance Absorption in Nitrogen

Author(s):
R. E. Morgado,
C. C. Cappiello,
M. P. Dugan,
C. A. Goulding,
S. D. Gardner,
C. L. Hollas,
G. J. Arnone,
L. E. Ussery,
J. M. White,
J. D. Zahrt

Submitted to:

DISCLAIMER

This report was prepared as an account of work sponsored by an agency of the United States Government. Neither the United States Government nor any agency thereof, nor any of their employees, makes any warranty, express or implied, or assumes any legal liability or responsibility for the accuracy, completeness, or usefulness of any information, apparatus, product, or process disclosed, or represents that its use would not infringe privately owned rights. Reference herein to any specific commercial product, process, or service by trade name, trademark, manufacturer, or otherwise does not necessarily constitute or imply its endorsement, recommendation, or favoring by the United States Government or any agency thereof. The views and opinions of authors expressed herein do not necessarily state or reflect those of the United States Government or any agency thereof.

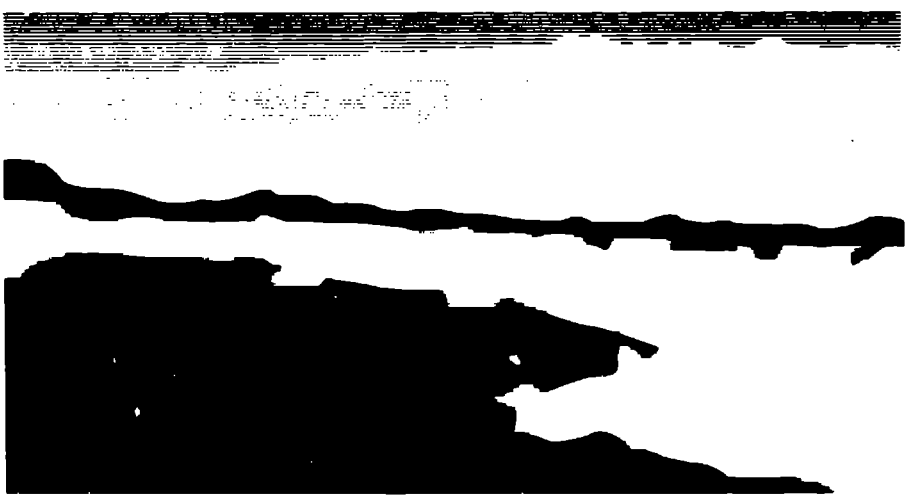

MASTER

Los Alamos
NATIONAL LABORATORY

Los Alamos National Laboratory, an affirmative action/equal opportunity employer, is operated by the University of California for the U.S. Department of Energy under contract W-7405-ENG-36. By acceptance of this article, the publisher recognizes that the U.S. Government retains a nonexclusive, royalty-free license to publish or reproduce the published form of this contribution, or to allow others to do so, for U.S. Government purposes. The Los Alamos National Laboratory requests that the publisher identify this article as work performed under the auspices of the U.S. Department of Energy.

Form No. 836 R5
ST 2629 10/91

DISTRIBUTION OF THIS DOCUMENT IS UNLIMITED

PROTOTYPE EXPLOSIVES DETECTION SYSTEM BASED ON NUCLEAR RESONANCE ABSORPTION IN NITROGEN

R. E. Morgado, G. J. Arnone, C. C. Cappiello, M. P. Dugan, S. D. Gardner,
C. A. Goulding, C. L. Hollas, L. E. Ussery, J. M. White, J. D. Zahrt,
Los Alamos National Laboratory, Los Alamos, NM 87545

B. L. Berman
George Washington University, Washington, DC 20052

R. W. Hamm, K. R. Crandall, and J. M. Potter
AccSys Technology, Inc., Pleasanton, CA 94566

R. A. Krauss,
Federal Aviation Administration, Atlantic City International Airport, NJ 08405

ABSTRACT

A laboratory protoype system has been developed for the experimental evaluation of an explosives detection technique based on nuclear resonance absorption of gamma rays in nitrogen. Major subsystems include a radiofrequency quadrupole proton accelerator and associated beam transport system, a high-power gamma-ray production target, an airline-luggage tomographic inspection station, and an image-processing/detection-alarm subsystem. The detection system performance, based on a limited experimental test, is reported.

1. INTRODUCTION AND BACKGROUND

In a feasibility study[1] completed in 1989, the determination of the nitrogen density in explosive simulants was demonstrated by imaging the object with a gamma-ray beam at an energy corresponding to a narrow nuclear resonance in nitrogen[2,3,4,5]. The study strongly suggested that certain explosives should be distinguishable from other inert materials commonly found in airline passenger luggage.

Based on these results, it was projected that a very high-current (≈15 mA) proton accelerator, would be necessary to generate the resonant gamma-ray flux to meet the Federal Aviation Administration (FAA) throughput requirement of 6s/bag. The eventual scope of the project was limited to a laboratory test of a reduced throughput, non-automated system. Although some of the major subsystems incorporated the design features of an airport prototype, e.g., the detector, array, data acquisition, and image processing subsystems, the accelerator and its subsystems were scaled back for a lower throughput rate by an order of magnitude. Nevertheless, the principal objective of the project, namely, an evaluation of many of the important operational characteristics of an airport system, was fulfilled.

In the following, we present the physical basis of the detection concept, a brief description of each major subsystem and its performance characteristics, and some results of our initial explosives detection tests. Preliminary conclusions on overall system performance are drawn.

This FAA-sponsored project was a collaboration between the Los Alamos National Laboratory (LANL) and the Soreq Nuclear Research Center (SNRC) of Yavne, Israel. Each collaborator produced a variant of the detector/luggage inspection system using a common accelerator/gamma-ray production system but different detection, interrogation and imaging concepts. The following describes the LANLapproach.

2. PHYSICAL BASIS OF THE DETECTION CONCEPT

The physical basis of the technique is a narrow energy state in the nucleus of ^{14}N that results in a strong resonance in the photonuclear cross section for the reaction $^{14}N(\gamma, p)^{13}C$ at 9.17 MeV. Gamma rays are absorbed by nitrogen, followed by the prompt emission of a proton and a ^{13}C nucleus. The transition rate from the ground state of ^{14}N is unusually large, and, as a result, 9.17-MeV gamma rays are highly absorbed, resulting in a strong indication of the presence of nitrogen.

The essential feature of our approach is the use of the inverse reaction[5], $^{13}C(p, \gamma)^{14}N$, to produce the gamma rays at the resonance energy. A 1.75-MeV proton beam incident on ^{13}C produces gamma rays at the resonance energy within a narrow angular interval with respect to the proton beam direction. As a result, desirable system characteristics are achieved: a fan beam of gamma rays of the correct energy from a localized source: a low level of radiation with no residual radioactivity, thus minimizing shielding: an efficient, inorganic scintillator detector is sufficient; and the required proton currents are attainable with available accelerator technology.

Gamma rays emitted by the recoiling ^{14}N nucleus in the above reaction are Doppler shifted and only those gamma rays emitted in an ≈ 0.7-degree-wide interval at 80.7 degrees from the direction of the proton beam are at the precise resonance energy. Thus, the locus of resonant photons is a narrow 80.7° conical section whose axis coincides with the proton beam.

The transmission of a resonant energy beam through a volume containing both nitrogen and other material is given by:

$$T_R = I_R/I_0 = \exp\left[-\left(f\sigma_R + \sigma_{NR}\right)\Delta m\right] \qquad 1$$

where I_R is the transmitted intensity, I_0 is the incident intensity, and, the total cross section is the sum of the resonance cross section, σ_R, averaged over the gamma-ray spectrum and that for the nonresonant processes, σ_{NR}; f is the mass fraction of nitrogen; and Δm the total mass thickness in atoms/cm^2. The non-resonant attenuation,

$$T_{NR} = I_{NR}/I_0 = \exp\left(-\sigma_{NR}\Delta m\right), \qquad 2$$

can be determined independently from transmission measurements at gamma-ray energies away from the resonance. Thus, the nitrogen mass thickness is

$$f\Delta m = (1/\sigma_R)\ln\left(T_{NR}/T_R\right). \qquad 3$$

In our case the off-resonance transmission is determined by including barium fluoride in the ^{13}C target, to produce 6.13-, 6.9-, and 7.1-MeV gamma rays from the (p,αγ) reaction in ^{19}F. Transmission measurements at these energies can be extrapolated to 9.17 MeV with sufficient accuracy to determine the nonresonant contribution to the total cross section. Transmission measurements through liquid nitrogen were used to determine the effective σ_R for the actual measurement system. A schematic of the detection concept is shown in Fig 1.

The technique is distinguished by the narrowness of the nitrogenresonance, its large integrated cross section (absorption probability), and its uniqueness to nitrogen, all of which result in high detection sensitivity and insensitivity to backgrounds. The 9.17-MeV gamma rays are very penetrating in ordinary matter, making it difficult to shield the explosives from detection. The technique is similar to x-ray imaging, but with notable exceptions: the image is of nitrogen alone; the probing radiation is very penetrating to all other elements; and overlying clutter that complicates the interpretation of conventional x-ray images is removed, simplifying the interpretation of the image and allowing for the possibility of automated detection.

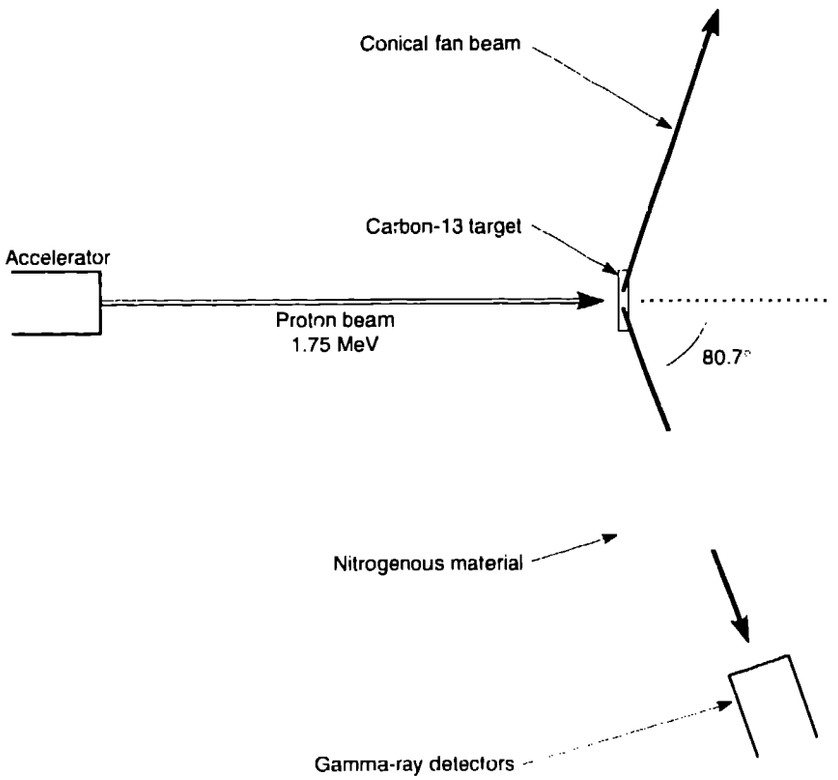

Fig. 1. Resonance-absorption-based detection concept.

3. THE PROTOTYPE DETECTION SYSTEM

The principal subsystems of the detection system are shown in Figure 2. A horizontal, pulsed beam of 1.75-MeV protons passes through a focusing quadrupole and energy debuncher, and is steered vertically downward by a combination bending and focusing magnet to produce a ≤1-cm-dia beam spot on the ^{13}C production target. The resulting fan beam of resonant gamma rays is approximately (within 10°) horizontal. Luggage is positioned on a platform that incrementally rotates 360° to produce multiple projections of a tomographic slice of the luggage. The luggage platform is elevated by a constant increment (the "slice" thickness) between successive rotational scans, until the vertical thickness of the bag has been scanned.

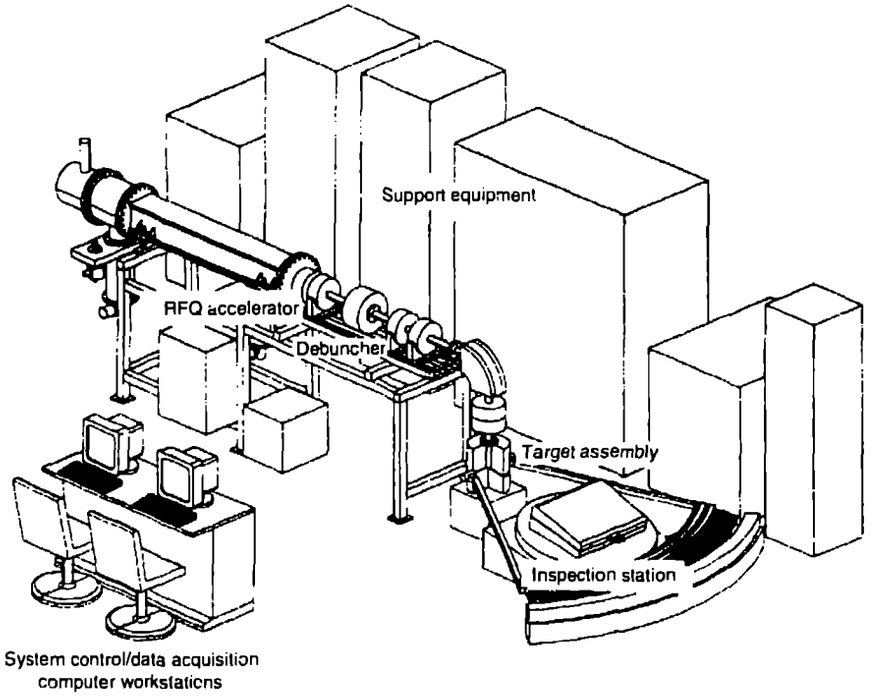

Fig. 2. Physical configuration of the detection system.

A collimated array of gamma-ray detectors is located at the resonant angle, spanning approximately one quadrant of the total fan beam. Individual detector signals are pre-processed, transmitted to a computer work station and temporarily stored. Upon completion of an inspection, the data are transmitted to a second computer work station for tomographic reconstruction of the luggage contents.

Two images are produced: a non-resonant image of the mass distribution at 6- and 7-MeV, and another of the nitrogen distribution using the resonant, 9.17-MeV gamma rays.

4. PROTON ACCELERATOR.C1.4. PROTON ACCELERATOR;

The proton source is a radiofrequency quadrupole (RFQ) linear accelerator, manufactured by AccSys Technology, Inc.,[7] modified and upgraded for resonance absorption applications. One objective of the project was to evaluate the suitability of a low duty factor RFQ linac for resonance transmission measurements relative to CW electrostatic accelerators. The principal issue centers on the beam characteristics typical of an RFQ accelerator, e.g., the effect of beam emittance and the micro and macro structures of the pulsed beam on detector performance. Other considerations are inherent beam stability, size and cost. These topics are the subject of a separate paper.[8]

5. PROTON TARGET

The most prominent design issue with respect to the proton target is its ability to withstand the heat load imposed by the high-current proton beam The original design requirement was for a 15-mA beam which was subsequently relaxed to a 0.5-1.0 mA beam. The targets used in these tests incorporated some of the features for the higher power levels. Target considerations include minimization of unwanted secondary gamma-ray production in the target backing and ease of fabrication.

A water-cooled copper backing was used to dissipate the heat. The water is transported through channels machined into the back of the target to within 1.6 mm of its front face. The channel is in the form of a logarithmic spiral (see Fig. 3), which produces a turbulent radial flow away from the central hot spot. Several coating variants were fabricated (see Table I) and tested. Excitation curves and gamma-ray spectra were obtained for a sample from each batch as a check on the thickness of deposited materials.

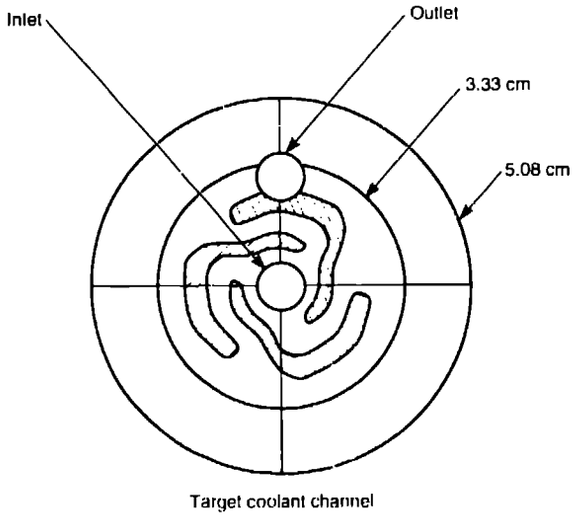

Fig. 3. High-power target design.

The Set # 1 duplicates our earliest design first tested in 1991 at power levels of ≤ 1 kW/cm^2 at the University of Birmingham (UK) Dynamitron CW accelerator. In the others, the ^{13}C thickness was increased to accommodate the inherent proton energy spread (estimated to be ≥ 20 keV) of an RFQ accelerator. The hafnium layers facilitate interlayer bonding; a layer of gold is necessary to degrade

the proton energy to that of the fluorine resonance level; and, in #6, the tantalum is to further degrade the proton energy to ≤ 500 keV, so that the gamma-ray background produced by the copper would be markedly lower. Coatings were applied by vapor deposition with a four-hearth electron-beam source. A quartz crystal monitor was used to control coating thicknesses. The final thicknesses and coating densities were determined from either profilometer measurements of witness plates or from microbalance differential weights.

No macroscopic degradation of these targets was observed in the course of operational testing of the detection system; however, the heat loading was only moderate (generally less than 2 kW over a period of ≤ 200 h).

Table I. Thick target coatings.

Target Set	Layer	Material	Thickness
#1	1	Carbon 13	148 μg/cm^2
	2	Hafnium	300 Å
	3	Gold	5750 Å
	4	Hafnium	300 Å
	5	Barium Fluoride	1300 Å
	6	Hafnium	300 Å
#2	1	Carbon 13	160 μg/cm^2
	2	Hafnium	500 Å
	3	Barium Fluoride	1300 Å
	4	Hafnium	300 Å
#3	1	Carbon 13	176 μg/cm^2
	2	Hafnium	300 Å
	3	Gold	5750 Å
	4	Hafnium	300 Å
	5	Barium Fluoride	1300 Å
	6	Tantulum	10 μm

6. LUGGAGE MANIPULATOR

The luggage manipulator sequentially elevates and rotates the luggage through the interrogating beam to produce the tomographic projections required for image reconstruction. The luggage manipulator rotates the bag in uniform increments through 360° for each vertical position. Upon completion of a rotational viewing sequence, the platform is raised or lowered by an amount determined by the beam width. This viewing sequence is repeated until the entire bag thickness is

The motion of the manipulator is controlled digitally from the data-acquisition computer work station. The number of rotational views and the viewing slice thickness are selectable operator input parameters. The duration of each view is determined by the number of detected gamma-rays; each view is continued until the desired number of counts is obtained. The desired counting statistics also is an operator input parameter.

7. GAMMA RAY DETECTOR SYSTEM

The optimization of detector parameters involved extensive computer modeling of detector response and experimental tests of different scintillator materials, geometries, and PMT coupling approaches. Bismuth germanate (BGO) was chosen on the basis of its stopping power (high Z), energy resolution (sufficient to resolve the 6- and 7-MeV resonance lines and the 9.17-MeV ^{14}N resonance), and stability (but requiring auxiliary temperature stabilization).

The detector slit width is ≈ 2 cm, as dictated by the angular width of the resonance photon beam. The resultant average pixel size is ≈ 2.0 cm x 1.3 cm. The 3-D spatial resolution of the viewing system is a function of these dimensions and the number of tomographic projections.

Several approaches for PMT optical coupling were investigated, but the most acceptable required tapering the BGO crystal to match the aperture of the PMT. The resultant crystal geometry is shown in Fig. 4. The custom-designed detectors were supplied by the Bicron Corporation. Sixty-four detector assemblies were required to span the lateral dimension of the inspection volume. The measured energy resolution of the detectors averaged ≈15% at 661 keV.

The detector mounting, collimator, and support stand were designed as an integral structure to support and align the BGO detectors and provide a 10-cm thick lead collimator slit. Figure 5 illustrates the assembled support system. Vitreous carbon spacers maintain the collimator slit spacing. Chilled-water lines were attached to the upper aluminum cover plate of the detector mounts to stabilize the scintillator crystal temperature at 17°C.

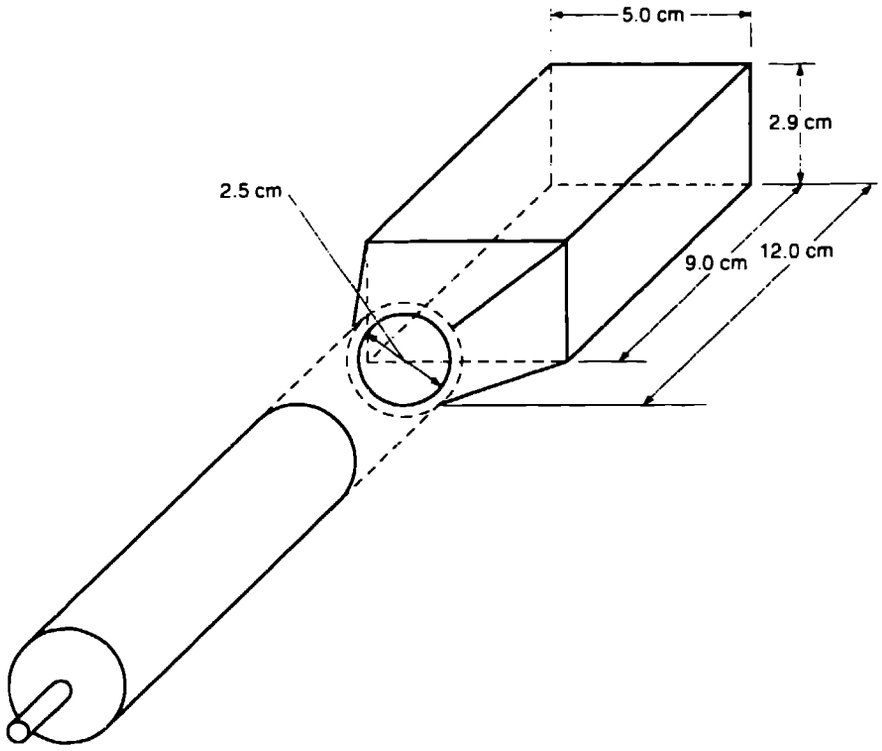

Fig. 4. Tapered BGO crystal and light pipe.

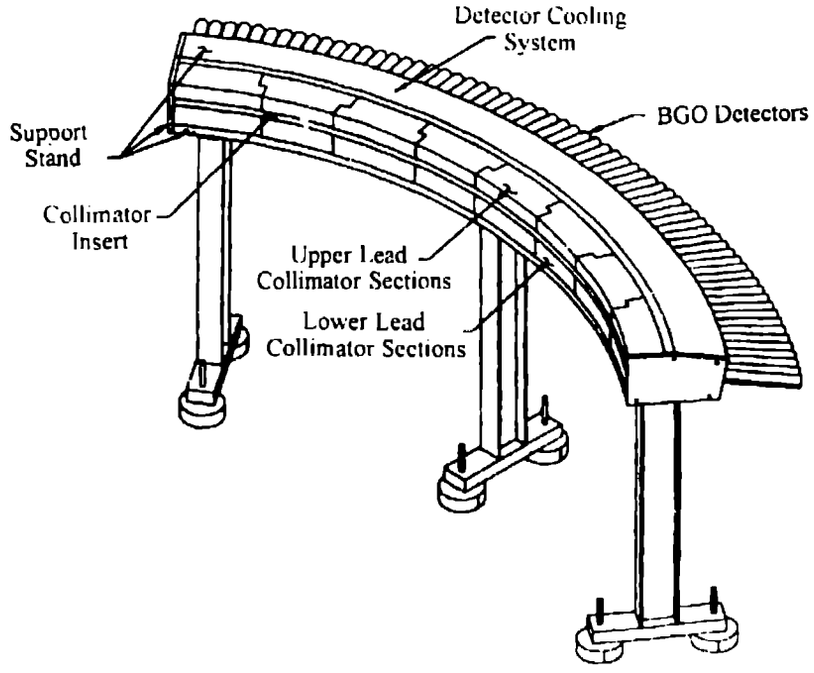

Fig. 5. Collimated detector array.

8. DATA ACQUISITION SYSTEM

The data acquisition system processes and categorizes the data according to detector location, inspection slice, and viewing projection, and stores the data for transfer to the image processing system. It also provides the hardware and software to control and monitor the luggage-inspection equipment, accelerator, and high-voltage supplies. The general design guidelines were: 1) provide near-real-time output (i.e., a process rate of $\approx 1.6\ 10^6$ events/s), 2) minimum dead time contribution, and 3) use commercial hardware and software when possible.

The selected system is VMEbus-based, with VxWorks (Wind River Systems) as the real-time operating system. The VMEbus protocol permits 21 or more CPUs per crate. All software development was done on a Sun SPARC II work station, which permits convenient downloading of software to each CPU as executable code.

9. TOMOGRAPHIC IMAGE PROCESSING

To detect irregularly-shaped explosives, a tomographic approach was chosen to provide a detailed 3-D mapping of the nitrogen density distribution within the luggage. Transmission measurements are also made at off-resonance energies, from which the total mass distribution within the luggage car be obtained as well. Although the nitrogen density alone can be a reliable signature, the combination of nitrogen density and total density clearly improves the accuracy of material identification, especially for cases involving marginal counting statistics.

At the current stage of development, the tomographic algorithm reconstructs a 2-D image of each slice. These are convenient for visual (non automated) interpretation of the images. The 2-D images can be displayed sequentially and, from interslice comparisons, the vertical locations of objects can be established. Although an initial version of a 3-D image reconstruction algorithm has been completed and partially tested, it has not been integrated into the system.

Images are reconstructed of both the total density distribution and of the nitrogen density distribution ("nitrograms"). The shape of higher density objects generally can be determined from the nonresonance image. Any objects with density outside the expected range for explosives ($\approx 1.0 - 1.9$ g/cm^3) are inferred to be a non explosive. Objects with densities within the above range are compared to the nitrogram image and if the nitogram indicates a significant nitrogen density at the corresponding location, the object is presumed to be an explosive. Automation of the preceding simple alarm protocol and others under consideration is not anticipated until an extensive image data base is available for evaluation and optimization of the system.

10. INITIAL DETECTION EXPERIMENTS

Testing of the system using live explosives began immediately upon completion of system assembly. Thus, the tests reported below are a part of the preliminary system optimization experiments and do not represent the expected capabilities of the system. Nevertheless, they provide an indication of the system's performance potential.

A blind-test demonstration was conducted by an FAA team in collaboration with explosives-development organizations at Los Alamos. A range of explosive types, densities, masses, nitrogen content, and shapes were assembled for these tests. Knowledge of the luggage contents was restricted

to the FAA team. A total of fourteen bags were inspected in these blind tests (the majority with explosives but some with explosives simulants), but the declared results of these are not yet available. However, a system calibration test can be reported, which was done in the same manner as the other tests, but with a piece of luggage containing known explosives and simulants. Although a very limited test, it provides an indication of the minimum potential capabilities of the technique.

Figure 6 shows a sketch of the calibration bag, its explosives contents, and the operational test parameters. The system calibration bag contains specimens representing four explosive types (see Table II) and geometries that range in total mass from 2/3 to 1 1/2 of the particular explosives threat for which the system was designed.

Table II. Test Explosives Physical Properties (nominal values).

Name	Principal Constituents	Density g/cm^3	^{14}N Density g/cm^3
Deta Sheet	75% PETN	1.5	0.19
Baratol	TNT/Bar$(NO_3)_2$	2.5	0.37
9205 PBX	92% RDX	1.7	0.59
Deta Sheet	63% PETN	1.5	0.17
9404 PBX	94% HMX	1.8	0.64

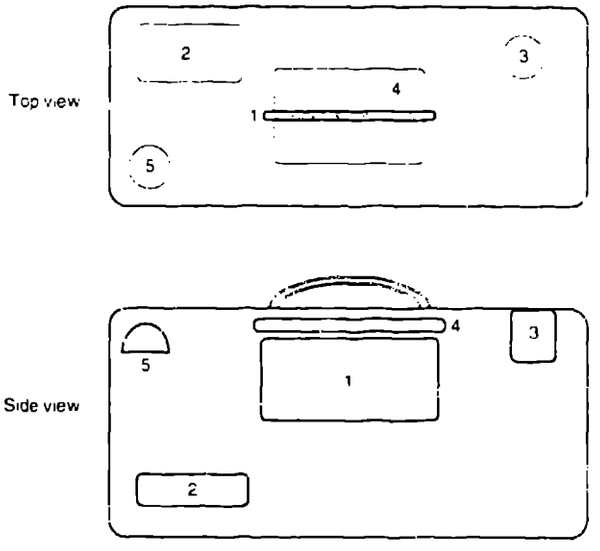

Fig. 6. Calibration-bag test parameters.

The explosive sheets are representative of the geometric extremes for practical explosive devices and, for this calibration test, were oriented approximately perpendicular and parallel to the viewing direction.

Image reconstructions of two of the slices near the top of the bag are shown in Fig. 7 that illustrate the detection capabilities and limitations of the unoptimized system in these first tests. The image pairs are from the nonresonance (left) and resonance (right) trans- mission measurements. The viewing perspective is from above the bag, looking downward (i.e., the top view in Fig. 6) and shows the density distribution over two selected horizontal cross sections (slices) of the bag. In these

reconstruction displays, the longitudinal axis of the bag is rotated clockwise approximately 45° from the top of the page.

Slice 2 is ~ 3 cm below the top of the bag, and at this level intersects test objects 3, 4, and 5 (see Fig. 6, side view). The upper, high density object (bright area) in the reconstructions is the 9205 PBX (seen in both slices) and the lower object is a hemispherically shaped 9404 PBX simulant (#5 in Fig. 6). The horizontal sheet explosive (#4) was not precisely parallel to the plane of plane of the beam, and slice 2 intersects only about 1/3 of the sheet. In the left hand reconstruction of slice 2, the diffuse, brighter region between and slightly to the right of test objects 3 and 5 is the portion of the sheet explosive (#4) noted above. The nitrogram of slice 2 clearly indicates the presence of high-density nitrogen in 3 and 5, but not for the sheet explosive (#4). However visual comparisons of successive slices in the original images marginally suggest the presence of nitrogen.

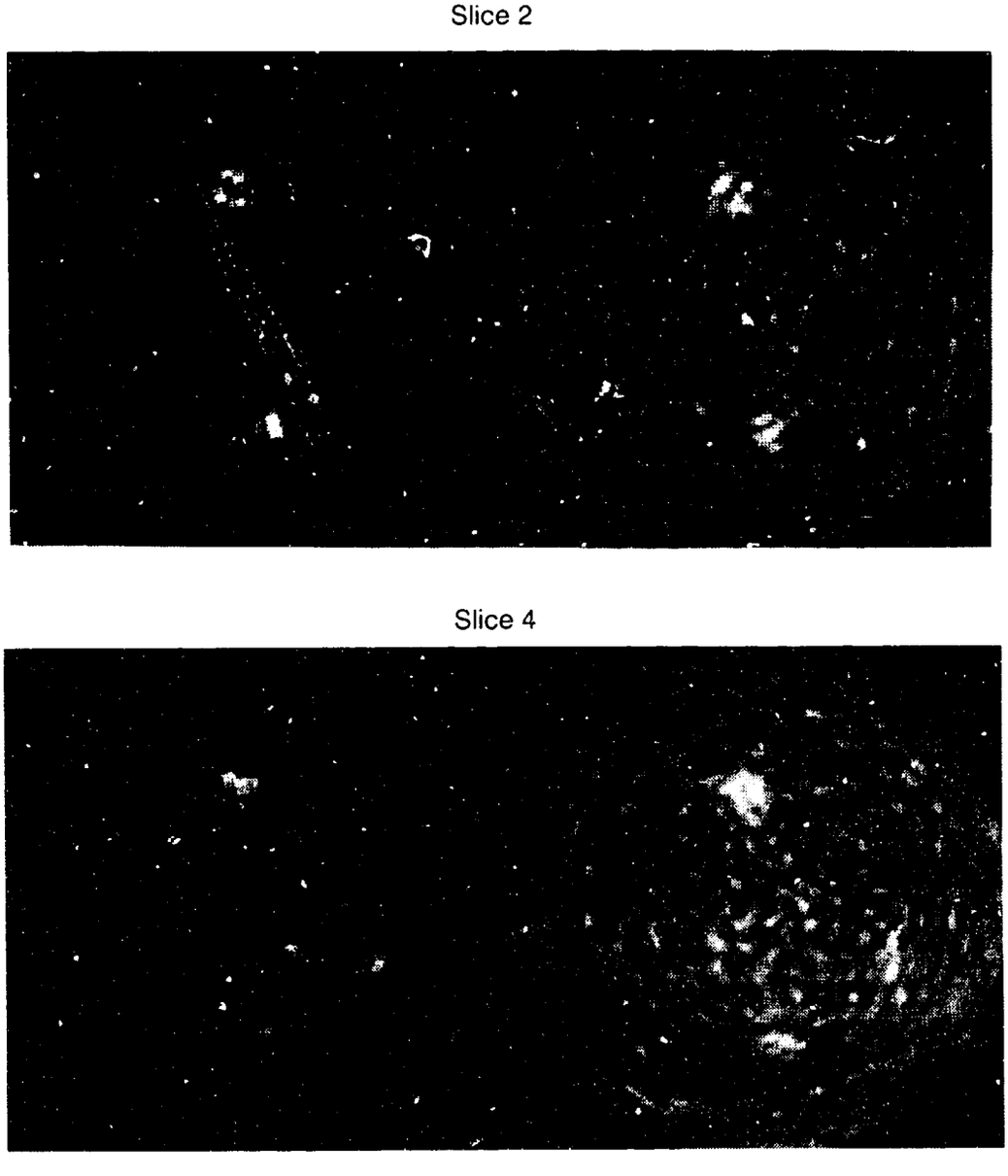

Fig. 7. Image reconstructions of the calibration bag.

In slice 4 (~5 cm below the top of the bag), the beam still intersects test objects 3 and 5, but now the vertical sheet (#1) has come into view. In the lower right quadrant of the reconstruction, a calibration standard positioned just outside the bag also has come into view. The vertical sheet (aligned with the longitudinal axis of the bag) can also be seen near the center of the nonresonance reconstruction. However, there is no indication of nitrogen associated with the sheet explosive. This result is not surprising, since the fundamental detectability limit of the system is directly related to the effective voxel size of the viewing system, and explosive samples with a dimension comparable to the minimum voxel dimension, as is the case for the sheet explosives, generally will appear as a lower density object (both total density and nitrogen density).

A 3-D tomographic approach was included in the system design concept, in part, to determine whether it would significantly improve detectability in the case of sheet explosives. However, 3-D imagery, and the associated special image processing techniques, is yet to be applied. Another known deficiency in the tested detection system is assosiated with the unoptimized beam transport system,which, because of an improperly focused proton beam, caused a reduction in the effective nitrogen cross section, which would also contribute to a lower apparent nitrogen density.

11. CONCLUSIONS

We conclude from this very limited test that a detection system based on this approach should readily detect nitrogen explosives in amounts well below our design objective, especially if they are in a compact geometry. We expect significant improvements from various system optimization measures and from the use of 3-D reconstructions. As these initial results suggest, these improvements will be necessary for detecting low-nitrogen-content explosives and sheet explosives. However, the actual detectability limits of this approach as well as the very important issue of false alarms cannot be addressed until system optimization is complete and an appropriate statistical data base acquired.

12. REFERENCES

1. The Feasib lity of Detecting FAA-Threat Quantities of Explosives in Luggage and Cargo Using Nuclear Resonance Absorption in Nitrogen, Phase I Final Report, October 1989, Los Alamos National Laboratory, Advanced Nuclear Technology, Internal Report.
2. Hannah, S.S. and Meyer-Schutzmeister, Luise, "Resonant Absorption by the 9.17-MeV Level in 14N", Physical Review 115, 4, (1959).
3. Biesiot, W. and Smith, Ph. B., "Parameters of the 9.17-MeV Level in 14N", Physical Review C 24, 6, (1981).
4. Vartsky, D., Goldberg, M. B., Engler, G., Goldschmidt, A., Breskin, A., Morgado, R. E., Hollas, C. L., Ussery, L.E., Berman, B. L., and Moss, C. E., "The Total Width of the 9.17-MeV Level in 14N," Nuclear Physics A505 (1989) 328-336.
5. Seagrave, John D., "Radiative Capture of Protons by 13C," Physical Review 85, 2, (1952).
6. AccSys Technology, Inc., 1177 Quarry Lane, Pleasanton, CA 94566.
7. R. E. Morgado, C. C. Cappiello, M. P. Dugan, C. A. Goulding, S. D. Gardner, C. L. Hollas, B. L. Berman, R. W. Hamm, K. R. Crandall, J. M. Potter, and R. A. Krauss, "The Effects of Proton-Beam Quality on the Production of Gamma Rays for Nuclear Resonance Absorption in Nitrogen," in *Proceedings of SPIE Substance Identification Technology Conference*, Innsbruck, Austria, October 1993, LA-12777-MS (May 1994).